Neurophysiologie Clinique/Clinical Neurophysiology (2014) 44, 479—490

ELSEVIER MASSON

Disponible en ligne sur
ScienceDirect
www.sciencedirect.com

Elsevier Masson France
EM|consulte
www.em-consulte.com/en

Neurophysiologie Clinique Clinical Neurophysiology

ORIGINAL ARTICLE/ARTICLE ORIGINAL

PureEEG: Automatic EEG artifact removal for epilepsy monitoring

Suppression automatique d'artefacts EEG pour le monitoring de l'épilepsie

M.M. Hartmann[a,*], K. Schindler[b], T.A. Gebbink[c], G. Gritsch[a], T. Kluge[a]

[a] *AIT Austrian Institute of Technology GmbH, Donau-City-Strasse 1, 1220 Vienna, Austria*
[b] *Department of Neurology, Inselspital Bern, Bern University Hospital, 3010 Bern, Switzerland*
[c] *University Medical Center Utrecht, Huispostnummer G03.131, Postbus 85500, 3508 GA Utrecht, Netherlands*

Received 20 June 2014; accepted 8 September 2014
Available online 26 September 2014

KEYWORDS
EEG;
Seizure;
Epilepsy;
Artifacts;
Automatic;
Artifact removal;
PureEEG

Summary
Aim of the study. — A novel method for removal of artifacts from long-term EEGs was developed and evaluated. The method targets most types of artifacts and works without user interaction.
Materials and methods. — The method is based on a neurophysiological model and utilizes an iterative Bayesian estimation scheme. The performance was evaluated by two independent reviewers. From 48 consecutive epilepsy patients, 102 twenty-second seizure onset EEGs were used to evaluate artifacts before and after artifact removal and regarding the erroneous attenuation of true EEG patterns.
Results. — The two reviewers found ''major improvements'' in 59% and 49% of the EEG epochs respectively, and ''minor improvements'' in 38% and 47% of the epochs, respectively. The answer ''similar or worse'' was chosen only in 0% and 4%, respectively. Neither of the reviewers found ''major attenuations'', i.e., a significant attenuation of significant EEG patterns. Most EEG epochs were found to be either ''mostly preserved'' or ''all preserved''. A ''minor attenuation'' was found only in 0% and 17%, respectively.
Conclusions. — The proposed artifact removal algorithm effectively removes artifacts from EEGs and improves the readability of EEGs impaired by artifacts. Only in rare cases did the algorithm slightly attenuate EEG patterns, but the clear visibility of significant patterns was preserved

* Corresponding author. Tel.: +43 50550 4229; fax: +43 50550 4125.
E-mail address: manfred.hartmann@ait.ac.at (M.M. Hartmann).

http://dx.doi.org/10.1016/j.neucli.2014.09.001

in all cases of this study. Current artifact removal methods work either semi-automatically or with insufficient reliability for clinical use, whereas the ''PureEEG'' method works fully automatically and leaves true EEG patterns unchanged with a high reliability.

MOTS CLÉS
EEG ;
Crise ;
Épilepsie ;
Artefacts ;
Analyse automatique ;
Suppression d'artefacts ;
PureEEG

Résumé
But de l'étude. — Une nouvelle méthode de suppression automatique d'artefacts dans les enregistrements électroencéphalographiques de longue durée a été évaluée. La méthode supprime la plupart des artefacts et fonctionne sans interaction de la part de l'utilisateur.
Méthodes. — La méthode est basée sur un modèle neurophysiologique et utilise un schéma itératif d'estimation bayésienne. La performance de l'algorithme a été évaluée par deux experts indépendants utilisant 102 enregistrements d'EEG ictal. Les experts ont évalué l'EEG avant et après la suppression d'artefacts en prêtant attention à une éventuelle atténuation du signal EEG d'origine cérébrale.
Résultats. — Les experts ont trouvé chacun dans 97 % et 96 % des cas une « amélioration considérable » ou une « amélioration faible » de l'EEG. La réponse « similaire ou pire » n'a été choisie que dans 0 % et 4 % des cas. Aucune « atténuation majeure » n'a été remarquée. La plupart des enregistrements ont eu l'appréciation « préservé en grande partie » et « complètement préservé ». Une « faible atténuation » n'a été trouvée que dans 0 % et 17 % des cas.
Conclusions. — Les méthodes actuelles de suppression d'artefacts ne fonctionnent que semi-automatiquement ou ne sont pas assez fiables pour les applications cliniques. La méthode proposée ici, « PureEEG », fonctionne tout à fait automatiquement et préserve de manière fiable le signal EEG d'origine cérébrale. PUREEEG supprime efficacement les artefacts dans les enregistrements EEG et améliore la lisibilité des EEG altérés par des artefacts. L'algorithme n'atténue le signal EEG d'origine cérébrale que dans de rares cas. En même temps, la visibilité est préservée dans tous les cas de cette étude.

Introduction

The electroencephalogram (EEG) is an important modality in the diagnosis of neurological disorders and the investigation of the functional properties of the brain. Unfortunately, EEG recordings are commonly contaminated by artifacts, potentials that do not originate from the brain but from various other sources [21,23]. Non-physiologic artifacts originate from various sources of electrical fields causing interference in the frequency band of EEGs. These sources include mains electricity noise at a frequency of 50 or 60 Hz, depending on the geographic region. Electric fields in external electronic devices, like mobile phones or implanted devices, like cardiac pacemakers also cause interference at frequencies relevant for EEGs. High-amplitude artifacts are often due to electromechanic machines, such as ventilators, feeding or infusion pumps or intravenous drips. The most common artifacts are caused by a faulty electrical connection of the electrodes and the skin of the patient [17], which is frequently a problem in long-term recordings. Patient movements often temporarily compromise this electrode-skin connection, giving rise to complex artifacts in the EEG. A second large group of artifacts have a physiologic origin. These comprise in particular ocular artifacts due to eye blinks and eye movements, which can be recognized by their characteristic waveforms and potential distributions in the EEG or by co-registration of an electrooculogram. Temporalis and frontalis muscles are the major source of myogenic artifacts, which may completely obscure an EEG recording due to their broad frequency spectrum and high amplitudes. Artifacts with a physiological origin also include cardiac artifacts, which can be identified by their correlation with the electrocardiogram, and also artifacts due to a cranial bone defect causing the so-called breach effect.

Although EEG artifacts may also give useful information, e.g. about the patient's state of vigilance or the occurrence of myoclonic jerks, they often lead to misinterpretation of the EEG as epileptiform, prompting incorrect treatment [1,22]. In addition to potential misinterpretation, artifacts often make EEGs difficult to analyze or even hardly readable, a problem that is particularly present in long-term recordings from epilepsy or ICU monitoring.

Correct identification of artifacts and interpretation of EEGs require application of EEG recording concepts [23]. Digital EEG and software-based review allow for post-hoc frequency filtering and montage selection, which might help to interpret impaired recordings. Artifact reduction using frequency filtering however requires that significant EEG patterns and artifacts are spectrally separate. Post-hoc montages may help if, e.g., a common reference electrode is impaired by artifacts.

The conventional post-hoc filtering and montage techniques are well established for clinical EEG review, but they have only a limited artifact-reducing power and must be adjusted frequently when recording conditions, artifact types and EEG patterns change. Numerous, more sophisticated computational methods have been proposed in the literature, aiming to identify, reduce or remove artifacts of various types from EEG recordings. The majority of these algorithms are based on blind source separation methods

[4,8], where the EEG is assumed to be a linear superposition of a number of components that can be divided into true EEG components and artifacts. In an unmixing step, separate components are calculated, artifactual components are identified and set to zero, and the remaining components are superimposed again leading to an EEG that should represent the true EEG without artifacts. The unmixing is typically based on Independent Component Analysis [11,24] and Principal Component Analysis [10,19]. The major drawback of these methods is that artifactual components must be identified, which is a non-trivial task for computational algorithms and usually has to be done manually by human experts. Fully automated procedures for artifact rejection have been proposed only rarely in the literature [13,14]. An interesting, spatio-temporal method is called Adaptive Filtering by Optimal Projection [2,3], which was evaluated very recently in [15] on a large dataset including 144 EEGs from epilepsy patients.

The major contribution of this article is a completely novel approach proposed for fully automatic artifact removal, called PureEEG. The major intention of the proposed method is to support the visual analysis of long-term EEG recordings. PureEEG rejects numerous types of artifacts that frequently obscure long-term recordings and impede their interpretation. More precisely, it targets artifacts that do not coincide with a spatio-temporal correlation pattern of an EEG of cerebral origin, which particularly includes artifacts due to myogenic contractions, faulty electrode-to-patient connections, patient movements and most non-physiologic sources. The method works fully automatically and without any patient-individual parameter adjustments, which also makes it well adapted as a pre-processor for all types of computational EEG analyses, such as electrical source imaging, automatic spike and seizure detection, or evoked potential analyses.

The algorithm is based on a neurophysiological signal model, which includes one term representing the pure EEG, which originates from cerebral sources only, and one term representing a wide range of artifacts. The model characterizes spatio-temporal correlations of the EEG and utilizes a Bayesian minimum mean squared error (MMSE) estimator for the separation of pure EEG components and artifactual components. An effective, iterative procedure is proposed for the critical characterization of a priori knowledge required by Bayesian estimators. In contrast to conventional frequency filtering, which operates in the spectral domain, and methods like Independent Component Analysis [24] and Principal Component Analysis [10], which operate in the spatial domain, the proposed approach separates the pure EEG and the artifacts in the spatio-spectral domain. The advantage is a high degree of freedom, which allows artifacts to be more accurately isolated and more precisely separated from the EEG, with only very low distortions of the pure EEG components.

The proposed method was developed as a pre-processor for computational analyses of EEGs from critically ill patients. In this article, it is shown that it yields a significant value for epilepsy monitoring units. We present the results of a validation study for visual review of ictal EEG recordings, which was accomplished by two independent reviewers using data from 102 seizures from 48 epilepsy patients.

Materials and methods

Spatio-temporal EEG signal model

The proposed method, PureEEG, is based on a stochastic, spatio-temporal model for EEGs, which are impaired by artifacts. The model includes K channels of digital EEG recordings, represented by length-K EEG vectors $e(t)$ with discrete time indices t. The EEG vectors $e(t)$ are decomposed into a superposition of three components,

$$e(t) = e_j(t) + e_a(t) + n(t) \tag{1}$$

where the pure EEG vectors $e_j(t)$ represent ''true EEG'' contributions from cerebral sources, the EEG artifact vectors $e_a(t)$ represent artifactual contributions caused by various types of artifact sources, and the noise vectors $n(t)$ contain noise due to amplification and analog-to-digital conversion and residual modeling errors.

The PureEEG artifact separation algorithm is based on a linear minimum mean square error (MMSE) estimator. This type of estimators requires a priori knowledge of second-order moments of observations and parameters to be estimated: it seems to be an obvious assumption, that the three components pure EEG e_j, artifacts a, and noise n are uncorrelated, meaning that their covariance is zero. Furthermore, it can be assumed, due to common high-pass filters in conventional EEG recording hardware, that all components are also zero-mean.

The full characterization of second-order moments in equation (1) would include all spatial and temporal cross-correlations, given by $C_{ej}(t, t')$.[1] However, this would lead to a computationally expensive MMSE estimator that could be hardly calculated in an acceptable amount of time for commonly used sampling rates and channel numbers. A significant reduction in complexity can be achieved, if the EEG is transformed into the frequency domain denoted by $\hat{e}(v) \triangleq \mathscr{F}e(v)$. We used a discrete cosine transform, which for real-valued EEGs has the advantage to be real-valued in the transform domain. Certainly, a discrete Fourier transform could also be used, which led to very similar results in our experiments. The frequency transform can be applied in the context of the overlap-add method [16], such that all assumptions and approximations must be valid only within each window separately. We applied the overlap-add method using Hamming windows and a distance of 1.5 seconds between succeeding frames. The linearity of $\mathscr{F}$ allows to transform each component separately, i.e., (1) can be written in the frequency domain as $\hat{e}(v) = \hat{e}_j(v) + \hat{e}_a(v) + n(v)$. In the frequency domain, we assume that spectral cross-correlations are approximately zero, i.e. $C_{\hat{e}j}(v, v') \cong \delta_{v,v'} C_{\hat{e}j}(v)$, $C_{\hat{e}a}(v, v') \cong \delta_{v,v'} C_{\hat{e}a}(v)$, and $C_{\hat{n}}(v, v') \cong \delta_{v,v'} C_{\hat{n}}(v)$. For discrete cosine transforms, this assumption would be exact for 1st-order Markov processes

[1] $E()$ denotes the expected value of an expression. Furthermore, we introduce the notations $\mu_x(t) \triangleq E(x(t))$ and $C_{x,y}(t, t') \triangleq E(x(t)) - \mu_x(t) \left(y^T(t') - \mu_y^T(t')\right)$ for the cross-correlation of vector-valued processes $x(t)$ and $y(t)$, furthermore, $C_x(t, t') \triangleq C_{x,x}(t, t')$ for the autocorrelation $x(t)$ and $C_x(t) \triangleq C_x(t, t)$ for the covariance matrix of $x(t)$.

[25] and asymptotically exact for finite-order Markov processes [7]. These are equivalent to processes obtained from autoregressive models, which have frequently been used in EEG signal processing methods [20]. Due to this simplification, the statistical characterization reduces to knowledge of covariance matrices $C_{\hat{e}j}(\nu)$ for the pure EEG vectors, $C_{\hat{e}a}(\nu)$ for the EEG artifact vectors, and $C_{\hat{n}}(\nu)$ for the noise vectors.

Characterization of the pure EEG component e_j can be based either on artifact-free EEG data or on a suitable data model. Artifact-free data can be cut into a sufficient number of samples and transformed into frequency domain in order to calculate, e.g., sample covariance matrices. It is possible to calculate specific covariance matrices for each individual subject, or averaged covariance matrices by mixing data samples from different subjects.

For the model-based approach, we make use of concepts established in the field of electrical source imaging. The task of calculating electrical sources corresponding to given potentials on the scalp, the so-called inverse solution, is typically based on a forward model, i.e., a linear mapping from source dipoles or source current distributions to electrical potentials on the electrode positions on the scalp. A forward model of this type will be used here for the characterization of spatial correlations of scalp potentials. Electrical source dipoles modeling EEG patterns of true cerebral origin are assumed to be uniformly distributed within a pre-defined brain-volume. The vector $j(t)$ includes all current densities represented by electrical dipoles at time t, which cause electrical potentials on the electrodes, denoted by $p_j(t)$. A description of this relation is given by the linear equation

$$p_j(t) = L_j(t) \tag{2}$$

where L is the so-called lead field matrix. Calculating suitable head models in terms of source spaces and lead field matrices has been treated extensively in the source imaging literature [12], where inverse problems are often poorly conditioned and strongly influenced by the forward model. In the algorithm proposed here, sources will not be localized and systems of equations will typically be well-conditioned. The choice of a specific method to determine a head model is therefore less important.

Each channel of an EEG recording is a difference of two electrode potentials. The pure EEG vectors $e_j(t)$ can thus be written as

$$e_j(t) = Mp_j(t) \tag{3}$$

where M is the $K \times L$ montage matrix, where each row represents an EEG channel and has ''+1'' and ''−1'' in the columns corresponding to the positive and the negative input electrodes, respectively. Since each EEG channel requires at least two input electrodes, the number of rows in M (i.e., the number of EEG channels) is typically lower than the number of columns (i.e., the number of electrodes). Computational re-referencing to a new reference or a common average reference could also be incorporated into the matrix M. However, this results in a rank-reduction of M and subsequently in a performance degradation of the artifact removal algorithm. Data should therefore always be used as recorded, without any post-processing. It should also be noted that M includes information about the reference electrode position, which unfortunately is not always documented in common EEG file formats. If the reference electrode position is not available, one can assume an ''infinitely remote'' position, corresponding to an all-zero row in the lead field matrix L, albeit with a decreased artifact removing performance.

Combination and frequency transformation of (2) and (3) results in $\hat{e}_j(\nu) = ML\hat{J}(\nu)$, i.e., the correlation matrix of $\hat{e}_j(\nu)$ can be written as

$$C_{\hat{e}}(\nu) = MLC_{\hat{j}}(\nu)L^TM^T \tag{4}$$

with a correlation matrix $C_{\hat{j}}(\nu)$ of source current densities j. It is assumed for simplicity that $C_{\hat{j}}(\nu)$ can be separated into a product

$$C_{\hat{j}}(\nu) = C^t_{\hat{j}}(\nu)\, C^s_{\hat{j}} \tag{5}$$

where $c^t_{\hat{j}}(\nu)$ and $C^s_{\hat{j}}$ characterize temporal and spatial correlations, respectively. This means that scalar function $c^t_{\hat{j}}(\nu)$, which defines the frequency-spectrum of j, is independent of the spatial position of a source dipole, i.e., all cerebral source dipoles are modeled with the same frequency spectrum. Conversely, the matrix $C^s_{\hat{j}}$ is modeled constant for all frequencies ν. This simplifying assumption will not be met in general. However, it leads to a significant reduction of the number of degrees of freedom in the model, which is important for the stability of the iterative prior estimation algorithm introduced in Subsection Iterative prior estimation. The second term to be characterized in the decomposition model (1) is the EEG artifact vector e_a. For this term, a simple model can thus be written as

$$e_a(t) = Ma(t) \tag{6}$$

where M is the montage matrix introduced in (3), and $a(t)$ is a length-L artifact vector that models all artifacts occurring at one or more electrodes. The montage matrix M in (6) incorporates the effects of artifacts on different electrodes: in contrast to normal electrodes affecting single channels, an artifact on a common reference electrode usually impairs all channels. In the frequency domain the correlation matrix $C_{\hat{e}a}(\nu)$ can be written as

$$C_{\hat{e}a}(\nu) = MC_{\hat{a}}(\nu)M^T \tag{7}$$

The correlation matrix $C_{\hat{a}}(\nu)$ is not known and hard to be characterized. It can be assumed however that the entries of a are uncorrelated, since many artifacts might be represented by single, independent components in a. This implies that $C_{\hat{a}}(\nu)$ can be assumed to be diagonal matrices. For the determination of the values of the diagonal elements, however, we refer to the iterative algorithm in Subsection Iterative prior estimation. The uncorrelated-property of artifactual components can be approximately justified for numerous artifact types, like those caused by faulty electrode connections and EMG artifacts. At least one can say that their cross-correlations are significantly smaller compared to the cross-correlations of the components in EEGs of cerebral origin. Note however that this assumption leads to an imperfect model for artifacts caused by eye blinks or eye movements, which typically show strong correlations across electrodes. As a consequence, ocular artifacts will hardly be removed by the proposed algorithm. For an artifact removal algorithm used for visual EEG review, this drawback should be acceptable, since ocular artifacts are most often easily recognized by an experienced EEG reviewer. Ocular artifacts usually do not significantly impair the visual interpretation of EEGs.

The third term to be characterized in model (1) is the noise vector n. It is assumed that the single entries in n are uncorrelated and that the noise is white with variance σ_n^2. This results in a noise correlation matrix $C_{\hat{n}}(v) = \sigma_n^2 I$.

MMSE artifact separation

Based on the EEG signal model introduced in Subsection Spatio-temporal EEG signal model, the pure EEG e_j can be separated from artifacts e_a using a linear minimum mean square error (MMSE) estimator, which might be the most important type of Bayesian estimators [9]. The linear MMSE estimator $e_j^*(t)$ minimizes the mean squared error $\varepsilon \triangleq E\left\{\left\|e_j^*(t) - e_j(t)\right\|^2\right\}$ and due to the assumption of uncorrelated pure EEG e_j, artifacts a, and noise n, it can be written as

$$e_j^*(t) = \mathscr{F}^+\left(C_{\hat{e}j} C_{\hat{e}}^{-1} \hat{e}\right)(t) \tag{8}$$

with an inverse frequency transform denoted by $\mathscr{F}^+(\cdot)$, the frequency domain EEG vector $\hat{e}(v)$ and its correlation matrix given by the sum

$$C_{\hat{e}}(v) = C_{\hat{e}j}(v) + M C_{\hat{a}}(v) M^T + \sigma_n^2 I \tag{9}$$

where $C_{\hat{e}j}$ from equation (4) and $C_{\hat{e}a}$ from (7) have been used. In a similarly way, a linear MMSE estimator for the artifacts a can be shown to be

$$a^*(t) = \mathscr{F}^+\left(C_{\hat{a}}(v) M^T C_{\hat{e}}^{-1}\right)(t) \tag{10}$$

An estimator for the artifact vector e_a can easily be calculated from (10) via multiplication with the montage matrix M. However, in the following subsection, we will make use of estimates for the artifact sources a directly rather than their effect on the EEG e_a.

Iterative prior estimation

The MMSE artifact separation method introduced in the previous subsection is a Bayesian estimator and thus requires some prior knowledge in terms of correlation matrices. In addition to the noise variance, these are covariance matrices of pure EEG sources j and artifact sources a. In Subsection Spatio-temporal EEG signal model, a spatio-temporal model for correlations of pure EEG sources was presented, but a priori artifact sources are unknown. The following procedure allows to iteratively estimate these prior information on artifactual components $a(t)$: using initial values for the artifact source covariance matrices $C_{\hat{a}}(v)$, an estimate $a^*(t)$ for the artifact sources can be calculated using equation (10). From this estimate, $a^*(t)$, an improved covariance matrix $C_{\hat{a}}(v)$ can be estimated, which then in turn again can be used in equation (10) for another update of the estimate $a^*(t)$. This iteration procedure can be continued until it converges, and finally the pure EEG estimate $e_j^*(t)$ is calculated via equation (8). The fact that $C_{\hat{a}}(v)$ is a priori unknown can be modelled by choosing very high initial values. Then, in the first loop of iterations, the MMSE estimator asymptotically becomes a simple least-squares estimator, which does not rely on a priori information [9]. The iterative algorithm quickly ''pulls down'' the continuously improving estimates for $C_{\hat{a}}(v)$. In our experiments, on numerous EEG samples this procedure always converged nicely after some tens of iterations.

Computational effort

As a tool for the visual analysis of long-term EEG recordings, it is important that the algorithm is computationally efficient. A reviewer looking through continuous EEG recordings and using an automatic artifact removal tool cannot wait for several seconds per page. We therefore implemented the PureEEG algorithm using Microsoft Visual C++ 2010 and Intel's Math Kernel Library 11.0. The implementation was furthermore optimized for speed by exploiting multi-core processing. The processing time for 10 seconds of EEG with artifacts was measured for various sampling rates and channel numbers. The speed tests were executed on a conventional Dell Notebook with an Intel® Core™ i5 at 2.50 GHz with 4 GB RAM and a 64 bit Windows 7 operating system. We evaluated the relationship between computational costs and sampling rates and channel numbers respectively.

Algorithm validation

Two EEG experts, an experienced epileptologist and a physician assistant with extensive clinical EEG experience performed the validation of PureEEG. We used EEGs from 102 seizures recorded during long-term epilepsy monitoring. From a series of 48 patients consecutively admitted to EEG monitoring, we took EEGs from the first three seizures respectively, which were either clinically or electrographically visible. Note that some patients had less than three seizures; the average number of seizures per patient used for this evaluation was 2.125. None of the validation data had been used for algorithm development, i.e., the PureEEG algorithm was no more modified after it was applied to these data for the first time. Data used for algorithm development were taken from different patients from epilepsy monitoring units or intensive care units. From each seizure one minute before and one minute after, seizure onset were presented to the reviewers. An epoch of twenty seconds was to be considered for the review. This epoch started five seconds before seizure onset and was visually marked in the data.

Reviewers were provided with EEG review software with standard features including post-hoc re-referencing, high pass-, low pass- and notch filtering. Additionally, this EEG review software included an implementation of the introduced PureEEG algorithm and a split-screen functionality, which allowed the reviewers to simultaneously see the EEG with and without PureEEG post-processing respectively. For each twenty-second epoch, the reviewers had to evaluate the amount of artifacts before and after PureEEG processing and the attenuation of EEG patterns after PureEEG processing. For each of the three questions, one out of four possible answers could be chosen. An almost equivalent evaluation scheme had been used for the evaluation of an artifact removal method in work of LeVan et al. [11]. The three questions and their possible answers were:

Table 1 Absolute numbers and proportion of seizures in each scoring category for both reviewers separately.

	Reviewer 1		Reviewer 2	
	n	%	*n*	%
What is the amount of artifacts before PureEEG processing?				
Almost none	12	11.8	3	2.9
Few	18	17.6	15	14.7
Significant	54	52.9	48	47.1
Considerable	18	17.6	36	35.3
What is the amount of artifacts after PureEEG processing?				
Mostly removed	3	3.3	0	0.0
Major improvement	53	58.9	49	49.0
Minor improvement	34	37.8	47	47.0
Similar or worse	0	0.0	4	4.0
Are EEG patterns attenuated after PureEEG processing?				
All preserved	20	19.6	23	22.5
Mostly preserved	65	63.7	79	77.5
Minor attenuation	17	16.7	0	0.0
Major attenuation	0	0.0	0	0.0

- question 1: ''What is the amount of artifacts before PureEEG processing?'' The reviewers were instructed to choose the answer ''Almost none'', if the amount of visually identified artifacts was negligible, ''Few'' if artifacts did not significantly obscure the EEG activity, ''Significant'' if a substantial amount of artifacts affected the EEG, and ''Considerable'' if a substantial amount of high-amplitude artifacts greatly affected long periods and multiple channels of the EEG;
- question 2: ''What is the amount of artifacts after PureEEG processing?'' Here, the reviewers should choose the answer ''Mostly removed'' if almost no artifactual pattern was remaining, ''Major improvement'' if previously obscured EEG patterns became notably easier to see, ''Minor improvement'' if previously obscured EEG patterns became slightly easier to see, and ''Similar or worse'' if no previously obscured EEG patterns became easier to see. If Question 1 had been answered with ''Almost none'', Question 2 did not have to be answered;
- question 3: ''Are EEG patterns attenuated after PureEEG processing?'' For this question we allowed the answers ''All preserved'' if all EEG patterns were preserved, ''Mostly preserved'' if all significant EEG patterns were preserved and only insignificant patterns might have been attenuated, ''Minor attenuation'' if some significant EEG pattern was attenuated, but still was clearly visible, and ''Major attenuation'' if some significant EEG pattern was significantly attenuated and was no more clearly visible.

Results

Expert validation

The results of the validation by the two reviewers are summarized in Table 1. The two reviewers rated the amount of artifacts before PureEEG processing as ''significant'' in 52.9% and 47.1% of the EEG samples, respectively, and as ''considerable'' in 17.6% and 35.3% respectively, which are more than two third of the samples in total. The bar diagrams in Fig. 1 illustrate the results of all three questions in percent for both reviewers separately.

After processing with PureEEG, a ''major improvement'' was found by the reviewers in 58.9% and 49.0% of the EEG epochs respectively, a ''minor improvement'' in 37.8% and 47.0% of the epochs. The answer ''similar or worse'' was chosen only by one reviewer in 4.0% of the samples. One of the reviewers rated ''mostly removed'' in 3.3% of the samples (cf. Fig. 1b). Although the algorithm does not remove artifacts completely, the quality of most seizure records was improved and become easier to interpret. One example for an EEG with artifacts, which were rated ''significant'' and ''considerable'' by the two reviewers respectively, is shown in Fig. 2 (top): shortly after seizure onset marked artifacts cover the majority of EEG channels. The resulting EEG after PureEEG processing can be seen in Fig. 2 (middle), which was a ''major improvement'' according to both reviewers. The EMG activity is strongly attenuated while the rhythmic, ictal patterns remain almost unaffected and became much easier to see, in particular in the last seconds of the epoch. In the spectrograms of channel P7-O1 before and after PureEEG processing at the bottom of Fig. 2 it can be seen that the strong artifacts in the raw EEG at the end of the epoch are greatly suppressed after PureEEG processing. Moreover, the EMG artifacts covering high frequencies during the whole epoch are also suppressed by the proposed algorithm. The rhythmic alpha activity on the other hand remains mostly unchanged, which demonstrates the capability of the algorithm of separating true EEG patterns from artifacts that do not exhibit the spatial and spectral properties as prescribed by the underlying model.

Neither of the reviewers found a ''major attenuation'', i.e., a significant attenuation of significant EEG patterns in any of the samples. This is an important result of the evaluation study, meaning that all significant EEG patterns remained clearly visible after PureEEG processing in all

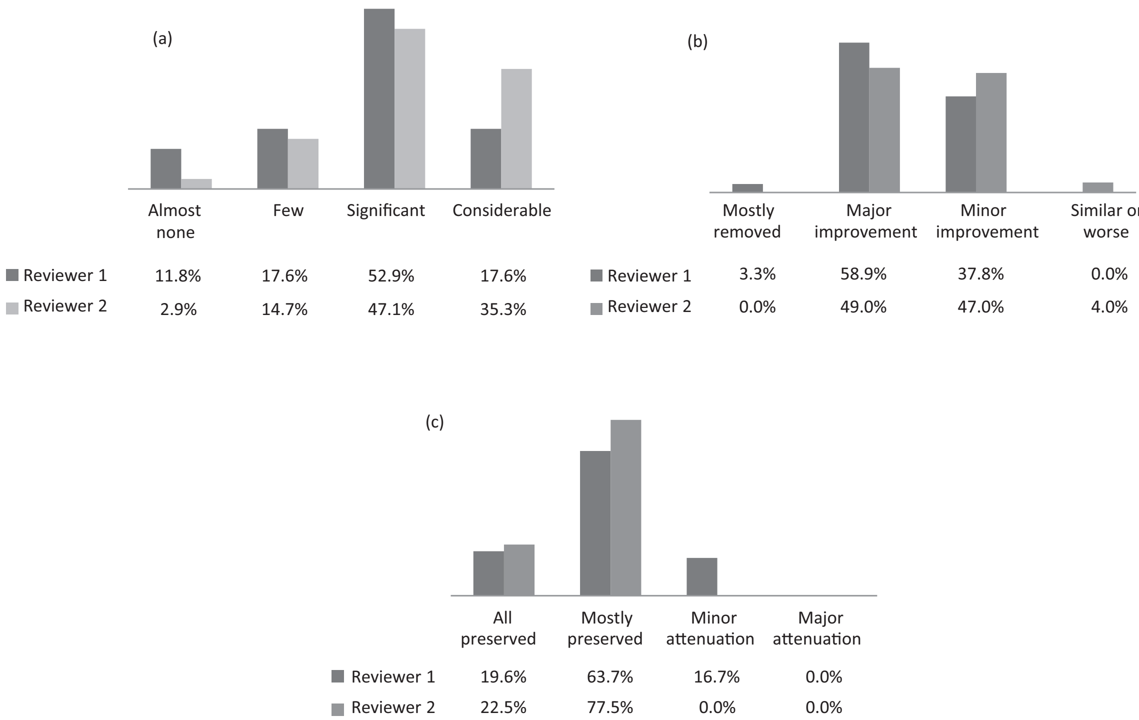

Figure 1 Bar diagrams illustrating the proporion of seizures in each scoring category for (a) the amount of artifacts before PureEEG processing, (b) the amount of artifacts after PureEEG processing, and (c) the attenuation of EEG patterns after PureEEG processing.

102 samples. One of the reviewers found minor attenuations in 16.7% of the samples. Fig. 3 (top) shows the EEG of one seizure containing strong artifacts, which cover large ranges of low- and high frequency bands. In the EEG resulting from PureEEG processing shown in Fig. 3 (bottom) one reviewer found a minor attenuation, and both reviewers concluded that there was a major improvement. This example shows that besides EMG artifacts PureEEG can simultaneously remove low-frequency artifacts, which probably have been caused by movements of the patient, and high-frequency artifacts of myogenic origin, while preserving the EEG to a great extent. The majority of EEG samples were rated with either ''mostly preserved'' or ''all preserved''. The answer ''mostly preserved'' was given in 63.7% and 77.5%, respectively, which means that all EEG patterns were preserved, and the answer ''all preserved'' was given in 19.6% and 22.5% of the seizures, respectively, which means that all significant patterns have been preserved.

The improvement of EEG quality due to PureEEG processing was evaluated within groups of EEGs with equal rating for the amount of artifacts in the raw EEG. The results are illustrated in Fig. 4. In the EEGs with considerable artifacts, i.e., the strongest level of artifact contamination, the reviewers found a major improvement or better in 70.4% of the samples and a minor improvement or less in 29.6% of the samples. In the EEGs with significant artifact contamination, the PureEEG algorithm was found to make a major improvement or better in 55.9% of the samples and a minor improvement or less in 44.1% of the samples. Here, at least a major improvement was achieved in more than half of the seizures. In 69.7% of the EEG samples with only few artifacts, the reviewers found either minor or no improvements, compared to 30.3% where the reviewers found major improvements or mostly removed artifacts. This is still an acceptable result, since in these samples the readability of the EEG was not significantly impaired even without artifact removal. For all EEGs with almost no artifacts, the improvements due to PureEEG obviously were ''minor or less''.

Improvements achievable in EEGs with only few artifacts hence are limited. But for increasing level of artifact contamination, where artifact removal becomes more and more important for the interpretation of EEGs, the PureEEG algorithm clearly improves the readability of an increasing amount of EEGs.

One ictal EEG epoch containing ocular artifacts due to eye blinks can be seen in Fig. 5. Moreover, it is affected by strong artifacts covering a wide range of frequencies at the begin and at the end of the epoch, a line noise artifact on the midline channels Cz-Pz/Pz-Oz, artifacts due to moving electrodes at right frontal positions, and repeated artifactual, very sharp transients at electrode F3. It can be seen, that the ocular artifacts remain mostly unchanged. This is an expected result, since the spatial correlations of ocular artifacts are closer to that of frontal EEG patterns than to that modeled by the artifact term in the underlying model of the PureEEG algorithm. The myogenic artifacts are significantly suppressed, the artifacts on right frontal electrodes and on F3 are mostly removed, and also the line noise, although it is clear that it could also be removed efficiently using a simple frequency filter.

Computational effort

The processing time for 10 seconds of EEG with artifacts was measured for sampling rates of 128 Hz, 256 Hz, 512 Hz, and

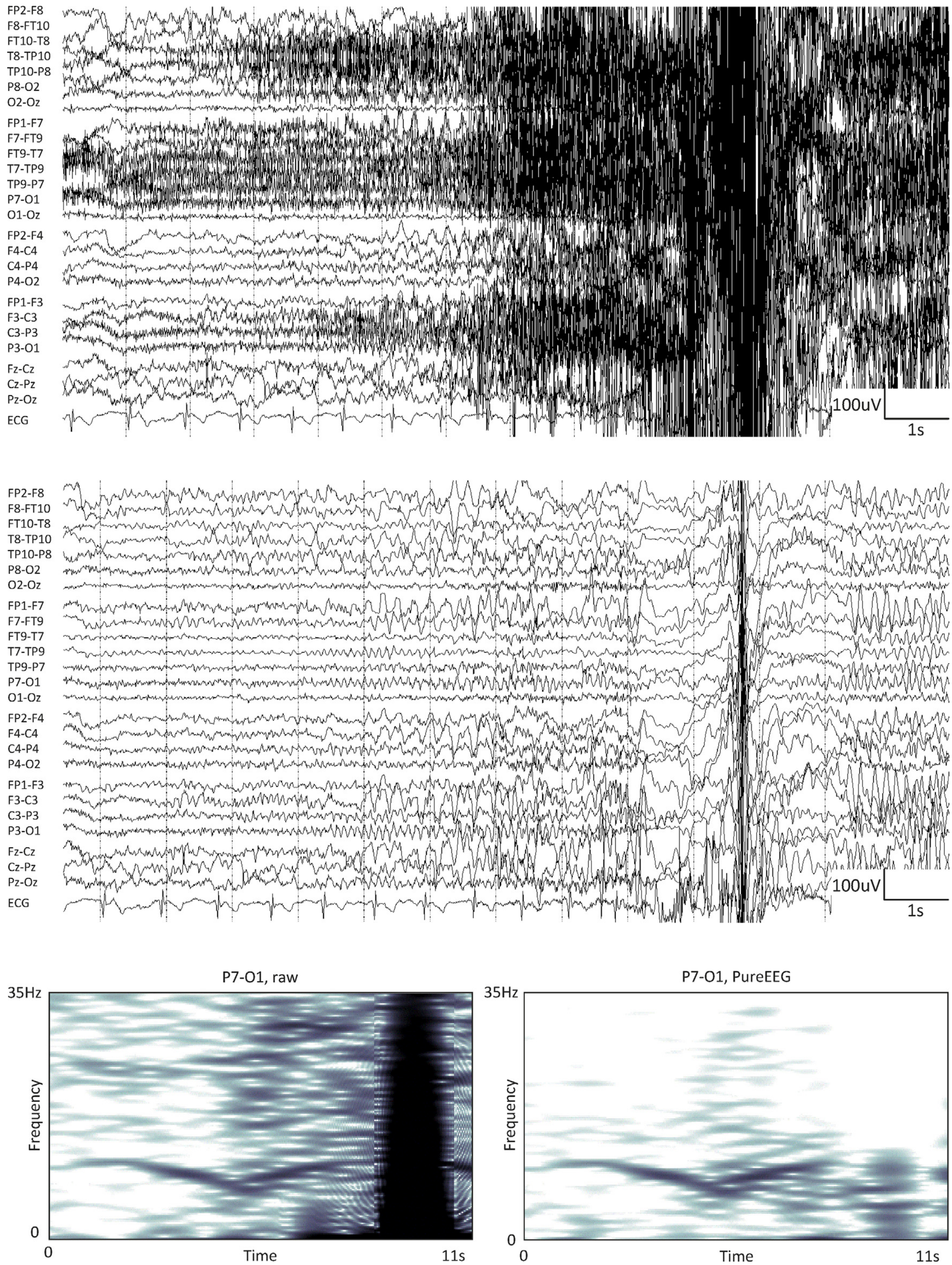

Figure 2 EEG sample #23. Significant artifacts in the raw EEG covering a large number of channels and several seconds (top). After PureEEG processing, a major improvement of the EEG quality and mostly preserved EEG patterns of cerebral origin can be seen (middle). Spectrogram of P7-O1 for EEG before (bottom left) and after (bottom right) PureEEG processing. The artifact at the end of the epoch, covering all frequencies, and the high-frequency artifacts covering the complete epoch are greatly suppressed after PureEEG processing. The rhythmic alpha activity at ~8 Hz remains widely unchanged.

1024 Hz, and for channel numbers of 9, 18, 36, and 72 channels. The results are shown in Table 2, where values between one and two seconds (for 10 s EEG) are shaded in light gray, and vales above two seconds are shaded in dark gray. In Fig. 6 the results are plotted in a line graph with logarithmic scales on both axes. It can easily be seen that computation time increases with both, sampling rate and channel number. We also made a trend analysis, which showed an almost linear

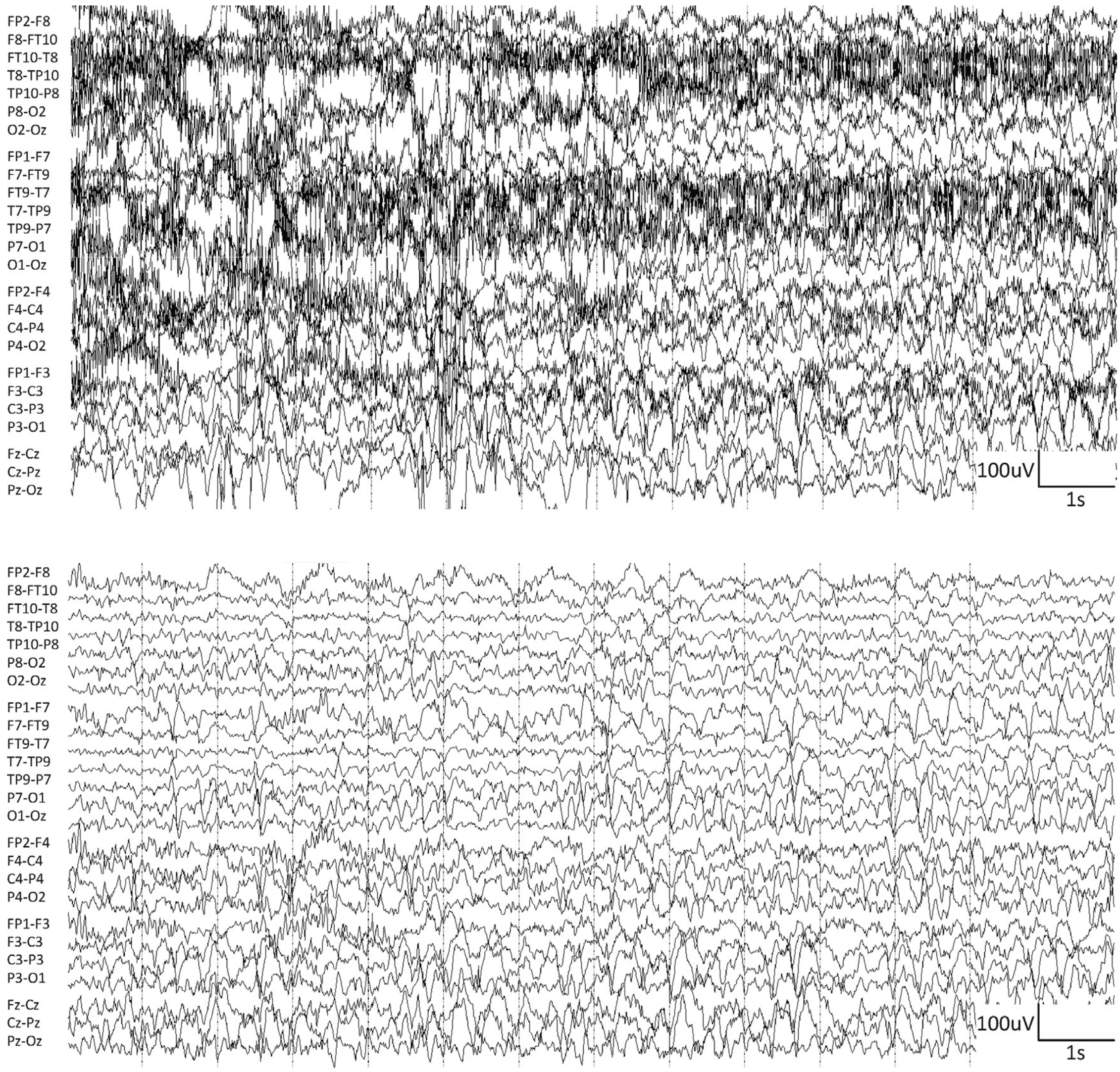

Figure 3 EEG sample #75. The raw EEG is covered by significant artifacts with low and high frequency components (top). After PureEEG processing, a major improvement of the EEG quality can be seen (bottom).

Table 2 Computation time in seconds for 10 seconds of EEG, which is about one typical EEG screen, for various sampling rates and channel numbers.

Sampling rate [Hz]	Number of channels			
	9	18	36	72
128	0.082	0.293	0.830	3.915
256	0.218	0.510	1.724	7.740
512	0.470	1.142	3.480	17.032
1024	0.893	2.225	7.532	36.008

relationship between processing time and sampling rate, and an increase of processing time with the 1.8th power of the channel number. The linear dependence of computational cost and sampling rate could be expected, since the number of samples is directly related to the number of frequencies v to be considered in the frequency domain. The dependency of computational costs with the 1.8th power of the number of channels might be a real limitation for high density EEGs. The reason for this can be found in equation (8), where a linear system of equation must be solved, which grows with the number of channels. It should be noted, that the absolute numbers clearly depend on the used hardware, the quality of the implementation, and also on the amount of artifacts that were to be removed, since the number of loops to be calculated is not fixed. However, the relation of computational costs and sampling rates or channel numbers remains valid and the evaluation at least demonstrates the order of computational costs to be expected.

Discussion

Model-based artifact removal

Artifact removal techniques for electroencephalography have been explored frequently in the literature. The demand for these techniques is high, since artifacts strongly deteriorate EEG review on the one hand and computational EEG

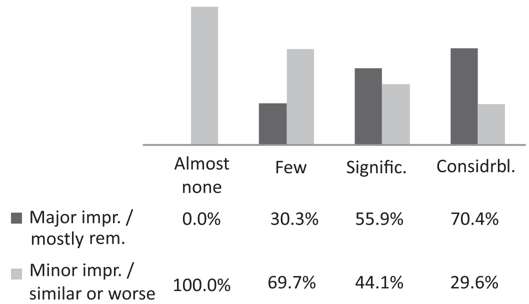

Figure 4 Artifact removal performance for various levels of artifact in the raw EEG. The more artifacts there are in the raw EEG, the greater is the improvement achieved by PureEEG. In 70.4% of EEGs with considerable artifacts, at least a major improvement was achieved.

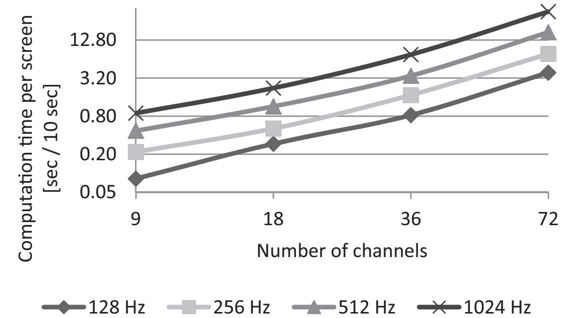

Figure 6 Computation time in seconds for 10 seconds of EEG as a function of the channel number for various sampling rates. The computational burden of the algorithm strongly depends on channel number and sampling rate.

processing on the other hand. Simple techniques such as frequency filtering can be used to reduce artifacts in EEGs, but their applicability is limited since frequency bands of artifacts usually overlap with EEG frequencies. Blind source separation (BSS) techniques such as principal component analysis [10] and independent component analysis [24] often yield promising results, but their major drawback is their demand for a manual selection of artifactual components to be removed. A few methods have been developed to facilitate this manual interaction [11], but fully automatic EEG artifact removal techniques have rarely been proposed [3]. So far, most commercially available EEG processing software does not offer satisfactory artifact removal features, although there would be a strong demand for it.

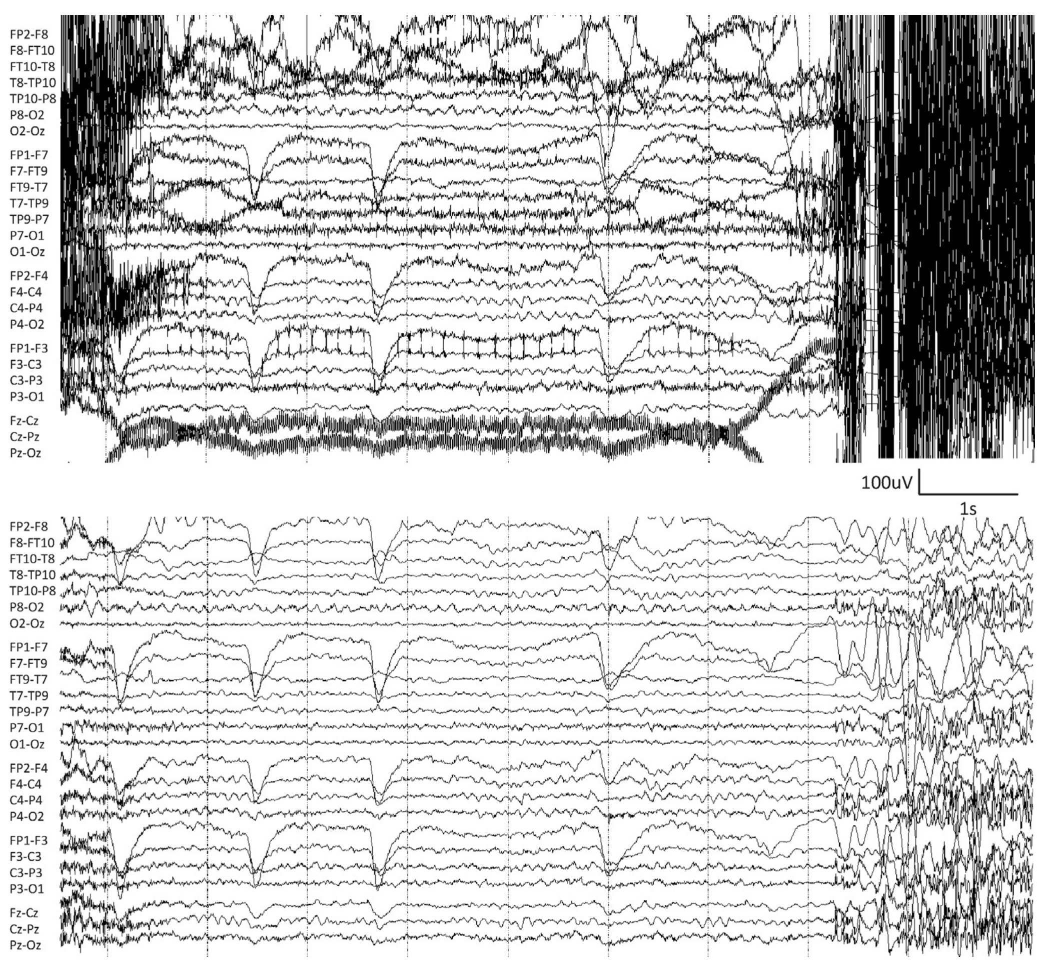

Figure 5 EEG sample #83. The raw EEG is covered by significant artifact including myogenic artifacts, movement artifacts, ocular artifacts, and line noise. After PureEEG processing, a major improvement of the EEG quality can be seen (bottom). Most artifacts, except from ocular artifacts, are significantly reduced.

The proposed PureEEG algorithm is a fully automatic approach. It does not require any user interaction for determination of artifacts. It is based on a neurophysiological signal model of EEG and artifacts and exploits knowledge about the positions of each electrode. Based on this model the algorithm is able to separate true EEG components from artifacts. The algorithm takes into account spatio-temporal correlations known from the model, which enables the separation of artifacts from pure, cerebral EEG. In contrast to purely spatial methods such as principal component analysis or independent component analysis [6], the ''unmixing matrix'' of the proposed algorithm depends on the frequency. Hence it is able to attenuate artifactual components only in the frequency range in which they occur, while EEG components in the same spatial subspace may remain unchanged in other frequency bands. In contrast, the unmixing matrix of purely spatial methods is always constant over frequency.

PureEEG exploits spatial correlations that are based on physiological modeling of the head and the electrodes on the skin. Temporal correlations of the artifacts are iteratively determined by the algorithm. Moreover the model includes the layout of the electrodes, such that the different effect of artifacts at normal electrodes in contrast to reference electrodes is also considered. This high level of details in the underlying model enables the excellent performance despite fully automatic operation.

Validation study

In the review of 102 seizures, two independent reviewers did not find any significant EEG pattern of cerebral origin that had been significantly attenuated by the PureEEG algorithm, i.e., all significant EEG patterns remained clearly visible after automatic artifact removal. This is a very important finding, since PureEEG is intended as a tool for the review of clinical EEG recordings. It could lead to misdiagnoses, if relevant EEG patterns would be missed due to an erroneous attenuation of true EEG components. PureEEG is also intended as a pre-processor for computational EEG analyses, where an irreversible attenuation of significant EEG patterns would deteriorate the accuracy of computational results. In the validation study the two reviewers found at least a major improvement due to PureEEG in 62.2% and 49% of the EEGs, respectively. One of the reviewers found at least a minor improvement in 100%, the second reviewer in 96% of the samples. Bearing in mind, that all significant EEG patterns remained clearly visible in 100% of the samples, the algorithm is a valuable tool for EEG review and reliably improves the quality of EEGs deteriorated by artifacts. After evaluation of 102 seizures, one of the reviewers summarized his impression of PureEEG as ''a very good tool that will give an added value to clinical practice'', and with PureEEG he ''could better recognize the first ictal EEG changes'' as compared to without PureEEG ''in the vast majority of EEGs''.

The automatic artifact removal algorithm proposed by LeVan and Gotman [11] was evaluated using the same protocol, such that a comparison of the two algorithms is possible in principle. However, it must be taken into account, that an evaluation by reviewers includes a strong subjective component and the validation datasets were not equal, such that comparisons must be made cautiously. One noticeable difference is, that the artifact removal was rated ''similar or worse'' in 25% of the seizures for the algorithm by LeVan, and in 0% and 4% of the seizures for the PureEEG algorithm. A ''major attenuation'' of true EEG patterns was found in none of the seizures with the PureEEG algorithm, but in 4% with LeVan's algorithm. On the other hand it is remarkable, that LeVan's algorithm preserved all true EEG patterns in 72.5% of the seizures, compared to the PureEEG algorithm, which preserved all true EEG patterns 20% and 22.5% of the seizures. Beyond the results of the validation it should be noted, that in contrast to LeVan's method the algorithm introduced here does not rely on training data, but on a neurophysiological model. The advantage hereby is that it does not require a new training if, e.g., the recording montage is changed. Due to the underlying model, which also includes the recording setup, the proposed algorithm automatically adapts to changes of the used electrode positions, montages, or sampling rates.

The proposed algorithm effectively removes several types of artifacts. This includes artifacts, which are characterized by clearly different spatio-temporal correlation patterns compared to true EEG activity of cerebral origin. This includes in particular artifacts of myogenic origin, due to faulty electrode connections, or electrode movements. In contrast, ocular artifacts are usually left unchanged. The reason for this is, that the potentials caused by eye movements or eye blinks exhibit spatial correlation patterns that are close to that of EEGs from frontal sources. For removal of ocular artifacts, BSS techniques have been shown to be effective [18], although they require relatively high signal-to-noise ratios [5]. The proposed algorithm however could be extended by additional components covering additional classes of artifacts.

Computational complexity

An important factor for the usability of an artifact removal algorithm is its computational burden. The acceptance of an artifact removal tool for EEG review could suffer significantly, if reviewers had to wait for several seconds for each EEG screen to be calculated. In our implementation, for standard EEG recordings with electrodes from the 10/20-system and a sampling rate of 256 Hz the algorithm required 0.5 seconds for processing 10 seconds of EEG, which clearly is an acceptable value. If the sampling rate is increased to 512 Hz, one has to wait for 1.14 seconds per screen, which will be acceptable for most users, but for even higher sampling rates, users would probably activate the algorithm only on demand, i.e., only when an EEG epoch is contaminated with strong artifacts impairing its readability. If the number of channels is increased to 36, the algorithm calculates for 1.72 seconds per screen. This might be still an acceptable value, but an additional increase of the channel number to 72, resulting in a computation time of more than seven seconds would be unfeasible for calculation on demand. In this case, and also in the case of very high sampling rates, a feasible operation mode could be to pre-calculate the artifact separation, although this would significantly increase memory demands. It should be noted however, that the targeted field of application is long-term monitoring, where artifacts are a major problem, but high density EEGs will probably remain an exception in the near future.

Conclusions

The proposed PureEEG artifact removal algorithm effectively removes artifacts from EEGs and improves the readability of EEGs impaired by artifacts. Only in rare cases does the algorithm attenuate EEG patterns slightly, but the clear visibility of significant patterns was preserved in all cases of the validation study. PureEEG is a valuable tool for EEG artifact removal, which reliably preserves significant EEG patterns from cerebral sources, and removes numerous types of artifacts, including myogenic artifacts, electrode artifacts, movement artifacts or line noise. A computationally efficient implementation of the algorithm makes it a viable alternative or extension to commonly used post-hoc frequency filtering in EEG review software.

Disclosure of interest

The authors declare that they have no conflicts of interest concerning this article.

Acknowledgements

This work was partly supported by The Austrian Research Promotion Agency grant 826816 (EpiMon).

References

[1] Benbadis SR, Tatum WO. Overintepretation of EEGs and misdiagnosis of epilepsy. J Clin Neurophysiol Off Publ Am Electroencephalogr Soc 2003;20(1):42—4.
[2] Boudet S, Peyrodie L, Forzy G, Pinti A, Toumi H, Gallois P. Improvements of adaptive filtering by optimal projection to filter different artifact types on long duration EEG recordings. Comput Methods Programs Biomed 2012;108(1): 234—49.
[3] Boudet S, Peyrodie L, Gallois P, Vasseur C. Filtering by optimal projection and application to automatic artifact removal from EEG. Signal Process 2007;87(8):1978—92.
[4] Fitzgibbon SP, Powers DMW, Pope KJ, Clark CR. Removal of EEG noise and artifact using blind source separation. J Clin Neurophysiol Off Publ Am Electroencephalogr Soc 2007;24(3):232—43.
[5] Ian Daly NN. Automated artifact removal from the electroencephalogram: a comparative study. Clin EEG Neurosci Off J EEG Clin Neurosci Soc ENCS 2013;44(4):291—306.
[6] Ille N, Berg P, Scherg M. Artifact correction of the ongoing EEG using spatial filters based on artifact and brain signal topographies. J Clin Neurophysiol Off Publ Am Electroencephalogr Soc 2002;19(2):113—24.
[7] Jain AK. A sinusoidal family of unitary transforms. IEEE Trans Pattern Anal Mach Intell 1979;PAMI—1(4):356—65.
[8] Jung T-P, Makeig S, Humphries C, Lee T-W, McKeown MJ, Iragui V. Removing electroencephalographic artifacts by blind source separation. Psychophysiology 2000;37(2):163—78.
[9] Kay S. Fundamentals of statistical signal processing, volume I: estimation theory. Prentice Hall; 1993 [1. Aufl.].
[10] Lagerlund TD, Sharbrough FW, Busacker NE. Spatial filtering of multichannel electroencephalographic recordings through principal component analysis by singular value decomposition. J Clin Neurophysiol Off Publ Am Electroencephalogr Soc 1997;14(1):73—82.
[11] LeVan P, Urrestarazu E, Gotman J. A system for automatic artifact removal in ictal scalp EEG based on independent component analysis and Bayesian classification. Clin Neurophysiol 2006;117(4):912—27.
[12] Michel CM, Murray MM, Lantz G, Gonzalez S, Spinelli L, Grave de Peralta R. EEG source imaging. Clin Neurophysiol Off J Int Fed Clin Neurophysiol 2004;115(10):2195—222.
[13] Mognon A, Jovicich J, Bruzzone L, Buiatti M. ADJUST: an automatic EEG artifact detector based on the joint use of spatial and temporal features. Psychophysiology 2010;48(2):229—40.
[14] Nolan H, Whelan R, Reilly RB. FASTER: fully automated statistical thresholding for EEG artifact rejection. J Neurosci Methods 2010;192(1):152—62.
[15] Peyrodie L, Gallois P, Boudet S, Cao H, Barbaste P, Szurhaj W. Evaluation of the AFOP/DAFOP method for automatic filtering of EEGs of patients with epilepsy. J Clin Neurophysiol 2014;31(2):152—61.
[16] Rabiner LR, Gold B. Theory and application of digital signal processing. Prentice-Hall; 1975.
[17] Reilly E. EEG recording and operation of the apparatus. Philadelphia, PA: Lippincott Williams & Wilkins; 2004. p. 139—59.
[18] Romero S, Mañanas MA, Barbanoj MJ. A comparative study of automatic techniques for ocular artifact reduction in spontaneous EEG signals based on clinical target variables: a simulation case. Comput Biol Med 2008;38(3):348—60.
[19] Schachinger D, Schindler K, Kluge T. Automatic reduction of artifacts in EEG-signals. In: 2007 15th International Conference on Digital Signal Processing; 2007. p. 143—6.
[20] Steinberg H-W, Gasser T, Franke J. Fitting autoregressive models to EEG time series: an empirical comparison of estimates of the order. IEEE Trans Acoust Speech Signal Process 1985;33(1):143—50.
[21] Stern JM. Atlas of EEG patterns. Philadelphia: Wolters Kluwer/Lippincott Williams & Wilkins Health; 2013.
[22] Tatum WO. Artifact-related epilepsy. Neurology 2013;80(Suppl. 1):S12—25.
[23] Tatum WO, Dworetzky BA, Schomer DL. Artifact and recording concepts in EEG. J Clin Neurophysiol 2011;28(3):252—63.
[24] Vigário RN. Extraction of ocular artefacts from EEG using independent component analysis. Electroencephalogr Clin Neurophysiol 1997;103(3):395—404.
[25] Yip P. Sine and cosine transforms. In: Poularikas A, Herausgeber, editors. The transforms and applications handbook. Second ed. CRC Press; 2000 [Internet, zitiert 2013 Aug 9] http://www.crcnetbase.com/doi/abs/10.1201/9781420036756.ch3